Alzheimer's & Dementia: Translational Research & Clinical Interventions 2 (2016) 69-81

Featured Article

Dissociation of Down syndrome and Alzheimer's disease effects with imaging

Dawn C. Matthews[a,*], Ana S. Lukic[a], Randolph D. Andrews[a], Boris Marendic[a], James Brewer[b], Robert A. Rissman[b], Lisa Mosconi[c], Stephen C. Strother[a,d], Miles N. Wernick[a,e], William C. Mobley[b], Seth Ness[f], Mark E. Schmidt[g], Michael S. Rafii[b], and for the Down Syndrome Biomarker Initiative and the Alzheimer's Disease Neuroimaging Initiative

[a]*ADM Diagnostics, Northbrook, IL, USA*
[b]*Alzheimer's Disease Cooperative Study, Department of Neurosciences, University of California San Diego School of Medicine, La Jolla, CA, USA*
[c]*Department of Psychiatry, New York University Langone School of Medicine, New York, NY, USA*
[d]*Rotman Research Institute, Baycrest Hospital and Medical Biophysics, University of Toronto, Toronto, Ontario, Canada*
[e]*Departments of Electrical and Computer Engineering and Biomedical Engineering, Medical Imaging Research Center, Illinois Institute of Technology, Chicago, IL, USA*
[f]*Janssen Research and Development LLC, Raritan, NJ, USA*
[g]*Janssen Pharmaceutica, Beerse, Belgium*

Abstract

Introduction: Down Syndrome (DS) adults experience accumulation of Alzheimer's disease (AD)–like amyloid plaques and tangles and a high incidence of dementia and could provide an enriched population to study AD-targeted treatments. However, to evaluate effects of therapeutic intervention, it is necessary to dissociate the contributions of DS and AD from overall phenotype. Imaging biomarkers offer the potential to characterize and stratify patients who will worsen clinically but have yielded mixed findings in DS subjects.

Methods: We evaluated 18F fluorodeoxyglucose positron emission tomography (PET), florbetapir PET, and structural magnetic resonance (sMR) image data from 12 nondemented DS adults using advanced multivariate machine learning methods.

Results: Our results showed distinctive patterns of glucose metabolism and brain volume enabling dissociation of DS and AD effects. AD-like pattern expression corresponded to amyloid burden and clinical measures.

Discussion: These findings lay groundwork to enable AD clinical trials with characterization and disease-specific tracking of DS adults.

Keywords: Down syndrome; Alzheimer's; Imaging; Amyloid; AV-45; Glucose metabolism; FDG; PET; MRI; Clinical trials; Prodromal; Biomarker initiative; DSBI; Classifier; NPAIRS

1. Introduction

Down syndrome (DS) is associated with an increased rate of Alzheimer's-like dementia, prevalent in up to 55% of individuals in their forties and 77% of age >60 years [1]. Neuritic plaques and neurofibrillary tangles consistent with Alzheimer's disease (AD) have been identified in nearly all DS adults examined of age >40 years [1,2]. Because of this, DS adults may provide a naturally enriched population

Data used in preparation of this article were obtained from the Alzheimer's Disease Neuroimaging Initiative (ADNI) database (adni.loni.usc.edu). As such, the investigators within the ADNI contributed to the design and implementation of ADNI and/or provided data but did not participate in analysis or writing of this report. A complete listing of ADNI investigators can be found at: http://adni.loni.usc.edu/wp-content/uploads/how_to_apply/ADNI_Acknowledgement_List.pdf.

*Corresponding author. Tel.: +1 847-707-0370; Fax: +1 847-223-5018.

E-mail address: dmatthews@admdx.com

http://dx.doi.org/10.1016/j.trci.2016.02.004

in which to evaluate the potential of pharmacological candidates to prevent AD progression. Ideally, trials would initiate treatment at a common, well-defined point before AD dementia [2]. This would require individual characterization of the degree of AD-related pathology and neurodegeneration distinct from DS effects. Detection of disease-modifying treatment effects would require distinguishing impact on AD-related pathology from that on underlying DS.

The primary objectives of our work were to: (a) dissociate within DS subjects the effects attributable to DS versus those associated with AD, and (b) to quantify the degree of AD progression. To pursue this, we applied multivariate analysis advances to baseline 18F fluorodeoxyglucose (FDG) PET structural magnetic resonance imaging (MRI) images and examined relationships with amyloid and clinical endpoints. We hypothesized that nondemented DS subjects with emerging AD would exhibit a pattern of neurodegeneration characteristic of prodromal AD. We postulated that standard image analysis methods might not be able to fully dissociate effects attributable to DS vs AD within subjects, and that multivariate analysis software capable of identifying different contributing networks or patterns to overall effect could isolate DS and AD components.

The source of DS data for our work was a 3-year DS Biomarker Initiative (DSBI) study was initiated by Janssen Research and Development in collaboration with the University of California San Diego (UCSD) and the Alzheimer's Disease Cooperative Study (ADCS). This study was designed to demonstrate methodology feasibility for a larger natural history trial. Endpoints include neuropsychological testing, positron emission tomography (PET) imaging of cerebral amyloid and glucose metabolism, MRI, and blood biomarkers [2,3].

In AD, a characteristic pattern of glucose hypometabolism emerges in hippocampus and posterior cingulate, expands to temporo-parietal regions, and gradually affects most cortical tissue, whereas pons, cerebellum, and motor and visual cortices are relatively preserved [4–6]. Changes are found in genetically at-risk individuals [7,8], begin years before symptom onset [9], and correlate with clinical decline [4,10]. In DS, results of FDG PET studies have been mixed [11]. Some studies in young adults (<25 years) have found no differences or only hypermetabolism compared to normals [12–14]. Other studies in DS adults have found hypometabolism in AD-relevant regions, more pronounced in demented than nondemented subjects [15–17]. Findings have not dissociated DS from AD effects within-subject nor quantified degree of AD progression.

AD also causes structural atrophy that initiates in entorhinal cortex, spreads to hippocampus, and expands to parietal and most cortical and subcortical structures [18–20], correlating with clinical progression [21,22]. In young DS persons (ages 5 to 23 years), MRI studies have shown reduced brain volume, shortened frontal lobes, reductions in cerebellum and brainstem, hippocampus, amygdala, and white matter but preservation of parietal and subcortical regions [23–25]. Studies in DS adults have found lower volumes overall and in cerebellum, cingulate gyrus, frontal lobe, superior temporal lobes, and hippocampi and associations between dementia, regional atrophy typical of AD, and ventricular enlargement [17,26–30]. However, structural effects of DS have not been dissociated within subject from those attributable to AD.

Consistent with postmortem findings, amyloid imaging studies in DS adults have found a high prevalence of AD-like amyloid associated with age and dementia [17,31–34].

Our work builds on these findings by differentiating, at the subject level, the effects attributable to DS independent of amyloid burden from those associated with emerging AD, and furthermore, provides a quantitative measure of the degree of AD progression. We demonstrate that these measures correlate with amyloid and clinical endpoints at baseline.

2. Methods

2.1. Subject selection

Twelve nondemented adult individuals diagnosed with DS, age 32–61 years, were enrolled. Exclusion of a diagnosis of dementia was based on absence of evidence of recent deterioration in cognitive function not secondary to medical illness (e.g., hypothyroidism, sleep apnea) or mental illness (e.g., depression), with absence of a significant decline in function over a period of 6 months or more. The diagnosing neurologist was experienced with premorbid deficits in DS and incorporated dementia diagnosis recommendations from the National Task Group on Intellectual Disabilities and Dementia Practices [35]. Ten subjects were female; six were *APOE* ε4 carriers. Assessments were conducted by UCSD in collaboration with the ADCS under IRB-approved protocols with patient informed consent [3].

2.2. Image data acquisition, processing, and analysis

All subjects received FDG PET, florbetapir (amyloid) PET, and structural MRI (sMRI) scans, acquired and processed as described in the Supplementary Material and [3]. FDG PET and MRI analyses were performed while blinded to amyloid, *APOE* ε4, and clinical status. Image analysis consisted of three parallel, complementary approaches.

2.2.1. Analyses with NPAIRS

The NPAIRS [36,37] multivariate analysis software framework was applied to detect patterns in FDG PET and T1-weighted sMRI characterizing similarities and differences between the DS group and pre-defined comparator groups. In brief, NPAIRS uses canonical variates analysis (a form of linear discriminant analysis) to identify uncorrelated spatial patterns that when mathematically combined account for overall variance across groups of image data. Importantly, NPAIRS uses an iterative resampling process

using split halves in which metrics of reproducibility (correlation between the model generated by each split half) and prediction (correct classification of the test half using the training half model) are used to optimize the model. This process addresses the issue of over-fitting that can arise in machine learning, particularly when data sets are small. A canonical variate (CV) score quantifies the degree to which each subject expresses each pattern. The test (rather than training) scores were used to report results.

For comparison to DS subjects in the NPAIRS analysis, four sets of 12 subjects (balancing N) were identified a priori from the Alzheimer's Disease Neuroimaging Initiative (ADNI) database based on ADNI clinical diagnosis, amyloid status, and age: amyloid negative (Am−) normal (NL), amyloid positive (Am+) AD, Am+ early mild cognitive impairment (EMCI), and Am+ late MCI (LMCI). The ADNI database (adni.loni.usc.edu) was launched in 2003 as a public–private partnership, led by Principal Investigator Michael Weiner MD, with the goal to test whether serial MRI, PET, other biological markers, and clinical and neuropsychological assessment can be combined to measure the progression of MCI and early AD (see www.adni-info.org). As DS FDG and MRI scans were acquired using ADNI protocols and processed in the same manner, comparison was feasible. Subjects were considered Am− if their amyloid PET cortical average standardized uptake value ratio (SUVR) was below a threshold of 1.47 for 11C-PiB [38] or <1.11 for florbetapir [39] or their cerebrospinal fluid (CSF) Abeta42 was >209 (allowing for threshold variability) and were considered Am+ if their amyloid PET SUVR exceeded threshold or their CSF Abeta42 level was <192 [40]. Given the relatively young DS subject ages, the youngest ADNI subjects meeting diagnostic and amyloid criteria were selected.

Three models using different combinations of classes were explored in NPAIRS using FDG PET, and the first was also explored using MRI: (1) DS, NL, AD; (2) DS, NL, AD, EMCI, LMCI; and (3) DS, NL. For each model of N classes, NPAIRS produced N-1 patterns and CV scores for each subject that quantified expression of each pattern.

In addition, because ADNI subjects were still somewhat older than most DS subjects, twelve age-matched, Am−, cognitively normal subjects (AE-NL) with FDG PET scans acquired at New York University [41] were selected for additional comparison in a four-class model of DS, NL, AD, and AE-NL. The purpose was to determine whether differences between DS and NL were consistent with that between DS and AE-NL. Acquisition parameters for these subjects were consistent with ADNI, and their processing parameters were sufficiently similar to enable confirmatory comparison as described in Results and shown in the Supplementary Material, but owing to other processing differences, they were not used as primary comparators. These differences included increased smoothing and the extent of superior slices in some scans, which were reconciled with additional smoothing and masking for analysis. The use of NYU subjects also helped to test for site differences.

Furthermore, because all DS scans but none of the comparator subjects came from a single site and scanner, an additional set of twelve ADNI subjects ranging in status from Am− NL to Am+ AD and having FDG PET scans acquired from the same site and scanner as the DS subjects were selected for comparison (SITE1 class). These subjects had not been selected as primary comparators because younger ADNI subjects were available. A model consisting of DS, NL, AD, and SITE1 was evaluated using NPAIRS to assess potential site differences, and ROI values of the SITE1 NL subjects were also compared to NL and DS.

2.2.2. AD progression classifier scoring

Each DS FDG PET scan was scored using our AD progression classifier. This algorithm, previously developed using machine learning and 166 subjects from ADNI characterized by clinical diagnosis, amyloid status, and longitudinal outcome, assigns a numeric score reflecting the degree to which the subject's scan expresses a pattern of hypometabolism and hypermetabolism relative to whole brain associated with AD progression [42] (See Supplementary Material and Supplementary Fig. 1 for further description.) DS CV scores were compared to mean scores previously derived from ADNI subjects at stages from Am− NL to Am+ AD.

2.2.3. Region of interest analyses

A priori AD-relevant regions of interest (ROIs) [43] were measured on the FDG scans, and SUVRs calculated. Primary regions of interest were posterior cingulate-precuneus (PCC) and inferior parietal cortex (IPL). Hippocampus, medial temporal gyrus (MTL; including hippocampus), lateral temporal cortex, and middle frontal gyrus were also examined. Whole brain without ventricles was used as the primary reference region, and SUVRs were compared using pons as an alternate reference region to further understand regional differences.

Once unblinded to amyloid data, each DS subject's amyloid cortical average SUVR was measured by averaging anterior cingulate, posterior cingulate, precuneus, lateral temporal, frontal, and inferior parietal regions, referenced to whole cerebellum. SUVRs were also calculated using pons and subcortical white matter as alternate reference regions for comparison, to confirm the absence of artifact in the primary reference region due to subject motion or technical factors during image acquisition.

2.3. Statistical analyses

Each NPAIRS analysis, through iterative split-half resampling, generated measures of reproducibility (correlation between the training model for each split half) and predictive power (correct classification of test split half using model developed by training split half) indicating whether results

were generalizable. Group CV scores were evaluated for normality and homogeneity of variance (Levene test), compared using nonparametric tests (Wilcoxon–Mann–Whitney) as the sample sizes were 12 or less per group, and effect sizes (ES) were calculated. In cases where all groups had at least 12 subjects and other criteria for parametric analyses were satisfied, parametric *t* tests were also performed for comparison. FDG PET ROI values for PCC and IPL referenced to whole brain were compared using nonparametric tests (Wilcoxon–Mann–Whitney) between the NL group and DS Am−, DS Am+, EMCI, LMCI, and AD groups, with and without age correction, and after applying a Bonferroni correction for multiple comparisons.

Correlation coefficients (nonparametric Spearman's R) were measured for FDG AD Progression scores, FDG CV scores, and sMRI CV scores vs age, amyloid SUVR, and baseline clinical measures; amyloid SUVRs vs baseline clinical measures; and sMRI-CV2 scores vs FDG AD Progression scores and $CV2_{FDG}$ scores.

3. Results

Subject demographics and DS participant clinical scores are shown in Table 1.

3.1. Amyloid status

Three DS subjects were Am− as measured using florbetapir PET, one was at threshold for positivity, and eight were Am+. Of the four Am− and threshold DS subjects, three were *APOE* ε3/ε3, and one (Am−) was 2/4. Five (62%) of the Am + subjects were heterozygous carriers (3/4) and three were non-carriers. Results referenced to whole cerebellum were consistent with those referenced to pons and subcortical white matter (Supplementary Fig. 2).

Table 1
Subject demographics

Variable	DS	NL	EMCI	LMCI	AD	AE-NL
Number	12	12	12	12	12	12
Age [Mean (SD)]	45 (8.5)	63 (2.5)	67 (2.1)	57 (3.2)	58 (2.5)	45 (8.5)
Gender (% F)	83	67	33	42	58	75
Education (y)	13 (5.1)	17 (2.0)	15 (2.6)	17 (2.5)	16 (2.7)	n/a
APOE ε4 carrier (%)	50	17	92	67	67	n/a
Amyloid pos (%)	58*	0	100	100	100	0

Vineland measures for DS subjects (adjusted to mental, rather than chronological, age)

Receptive	12.58 (3.65)	Expressive	12.83 (3.74)
Written	15.73 (5.00)	Personal	14.58 (4.08)
Domestic	18.09 (3.45)	Community	15.67 (4.40)
Interpersonal relationships	15.50 (3.63)	Play and leisure time	12.67 (5.48)
Coping skills	17.33 (3.23)		

*DS amyloid burden as measured during analysis; negative includes one subject at or just below threshold depending on the reference region applied.

3.2. FDG NPAIRS comparisons

Results of the NPAIRS 3-class comparison of DS, NL, and AD are shown in Fig. 1. Two distinct glucose metabolism patterns with partial overlap were identified, each having reproducibility and prediction metrics indicating generalizability to a broader population (as did all patterns discussed). The first pattern (Fig. 1A, $CV1_{FDG}$) differentiated DS from NL ($P < .00001$, effect size (ES) 5.94) and AD ($P < .00001$, ES 6.58). There was no separation between Am− and Am+ DS subjects ($CV1_{FDG}$ plot, Fig. 1A). This pattern did not correlate with age. The second (Fig. 1B, $CV2_{FDG}$) separated NL from AD ($P < .00001$, ES 3.48), whereas DS scores were distributed across the range from NL to AD. All Am− or threshold subjects had $CV2_{FDG}$ scores in the range of NL. $CV2_{FDG}$ correlated with age in DS subjects ($R = 0.659$, $P < .02$). (Results were consistent using both parametric and nonparametric tests.)

In the DS-associated pattern $CV1_{FDG}$, hypometabolism was observed in posterior cingulate, anterior cingulate, precuneus (particularly anterior), paracentral lobule, postcentral gyrus/supplementary motor cortex, superior temporal cortex, hippocampus, striatum, insula, and inferior frontal cortex. Relative hypermetabolism was found in frontal cortex, superior temporal gyrus, and occipital cortex. Pattern features are relative to brain mean; therefore, hypermetabolism or volume increases can also be interpreted as relative preservation.

The $CV2_{FDG}$ pattern (Fig. 1B) was characterized by hypometabolism in posterior cingulate, posterior precuneus, inferior parietal cortex, lateral temporal cortex, and prefrontal cortex. Relative hypermetabolism was found in cerebellum, pons, paracentral lobule, putamen, thalamus, and occipital subregions. The $CV2_{FDG}$ and $CV1_{FDG}$ patterns overlapped in a portion of precuneus and posterior cingulate, but otherwise were largely distinct (Supplementary Fig. 3).

The 5-class NPAIRS analysis of DS, NL, EMCI, LMCI, and AD subjects provided a finer resolution comparison of DS subjects to the AD progression spectrum. The five-class CV1 pattern was similar to the three-class $CV1_{FDG}$ pattern, differentiating DS from all other groups ($P < .00001$, ES 6.38) and did not differentiate non-DS groups. An AD-like CV2 pattern showed cascade-like progression from NL to EMCI to LMCI to AD as we have found in our AD Progression classifier. DS subjects scored across the spectrum from NL to AD as in the 3-class comparison (Supplementary Fig. 4).

Confirming that the DS-associated pattern $CV1_{FDG}$ was not attributable to DS vs. ADNI subject age differences, the 4-class NPAIRS analysis of DS, NL, AD, and AE-NL subjects produced a CV1 pattern differentiating DS similarly from both NL and AE-NL, highly similar to the 3-class $CV1_{FDG}$ pattern. In addition, a CV2 pattern differentiated AD subjects from Normal groups (both ADNI and NYU), with DS subjects expressing a spectrum of scores. Despite lower resolution due to greater smoothing, the absence of superior slices, the CV1 and CV2 eigenimages were very similar to those produced using only ADNI comparators (Supplementary Fig. 5).

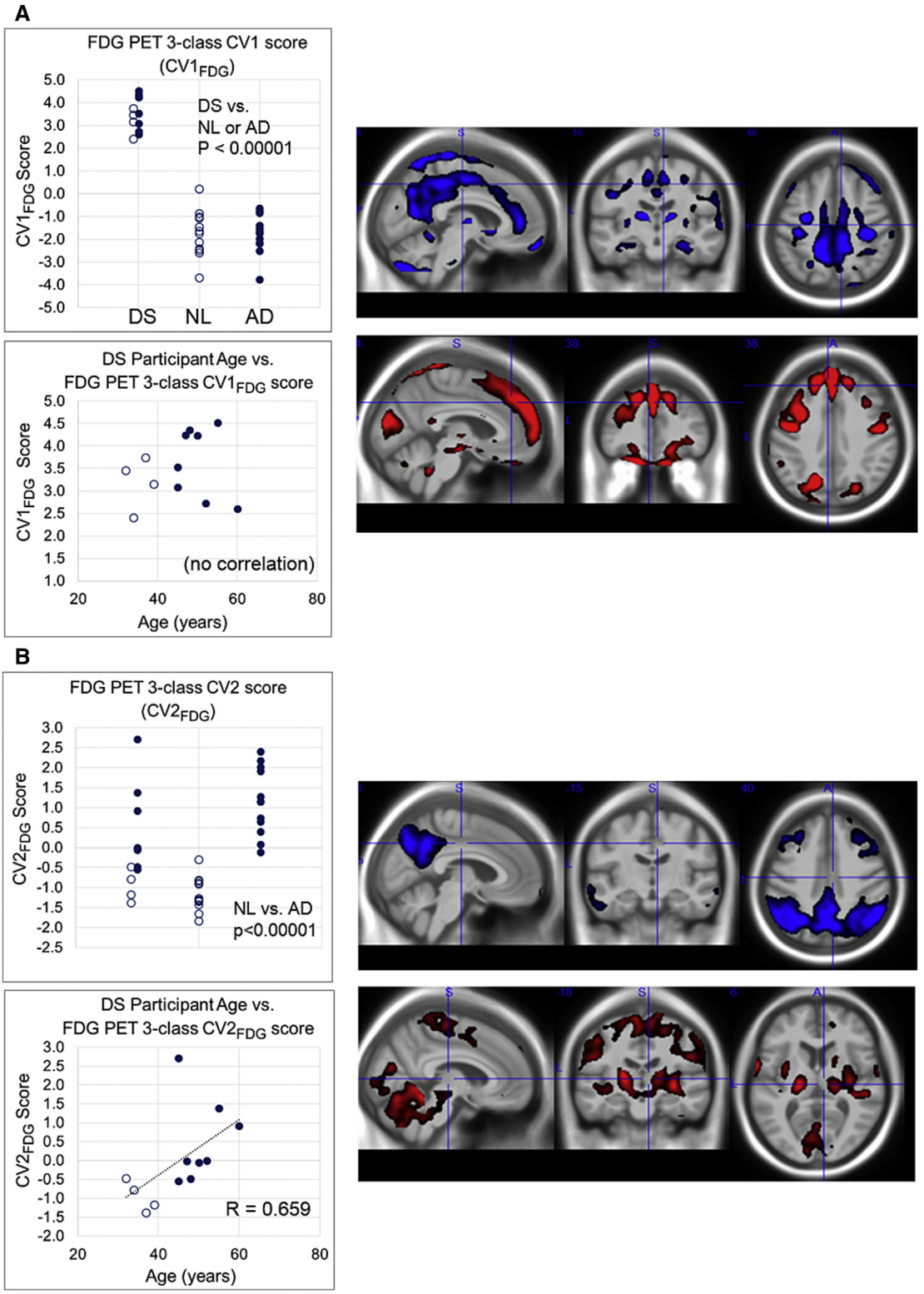

Fig. 1. Results of 3-class FDG PET NPAIRS analysis. (A) DS-specific ($CV1_{FDG}$) and (B) AD-specific (differentiates AD vs NL, $CV2_{FDG}$) patterns are shown from the three-class FDG PET analysis. The numeric scores (circles) in the graph reflects the degree to which each subject expresses the corresponding pattern of relative hypo (blue) and hyper (red) metabolism (higher score on y-axis corresponds to greater pattern expression). Unfilled circles indicate amyloid negative or threshold, and filled circles indicate amyloid positive. DS subjects who were amyloid negative or at threshold as measured by florbetapir PET are shown as unfilled circles to the left of those who were amyloid positive (filled circles). Abbreviation: FDG, fluorodeoxyglucose; PET, positron emission tomography; DS, Down syndrome; AD, Alzheimer's disease; NL, cognitively normal amyloid negative.

Suggesting that the DS differences were not site-related, the 4-class analysis of DS, NL, AD, and SITE1 produced a CV1 pattern resembling the 3-class $CV1_{FDG}$ pattern and differentiating DS from NL, AD, and SITE1 (all $P < .00001$, Supplementary Fig. 6), which were not distinguished from one another. CV2 and CV3 patterns differentiated NL and AD ($P < .00001$, $P < .0001$), with DS and SITE1 subjects distributed in expression.

The 2-class analysis comparing DS and NL subjects was constrained to identify only one pattern. This pattern differentiated DS and NL and incorporated elements from both $CV1_{FDG}$ and $CV2_{FDG}$. Similar to published studies, contributions of DS and AD could not be dissociated (Supplementary Fig. 7).

3.3. FDG AD progression classifier scores

DS AD Progression scores (Fig. 2A) ranged from values typical of Am− NL subjects to those of AD subjects established through previous independent testing of ADNI subjects of known clinical diagnosis and amyloid status. AD Progression scores increased with age (R = 0.602, $P < .04$) and with amyloid burden. All Am− or threshold subjects had scores reflecting less AD-like pattern expression than typical of LMCI or AD.

Shown in Fig. 2B and 2D, the $CV2_{FDG}$ scores correlate with FDG AD progression scores (R = 0.993, $P < .00001$), and the pattern is highly similar to the a priori AD progression pattern, dominated by hypometabolism in posterior cingulate, precuneus, and inferior parietal cortices with preservation in cerebellum, pons, paracentral lobule, thalamus, and striatum.

3.4. FDG region of interest analyses

Fig. 3A and 3B present region of interest analysis results in PCC and IPL, referenced to whole brain, for DS Am−, DS Am+, NL, EMCI, LMCI, and AD subjects. Fig. 3C and 3D show the relationship between SUVR and age for DS, NL, and AD. Consistent with the PCC hypometabolism observed

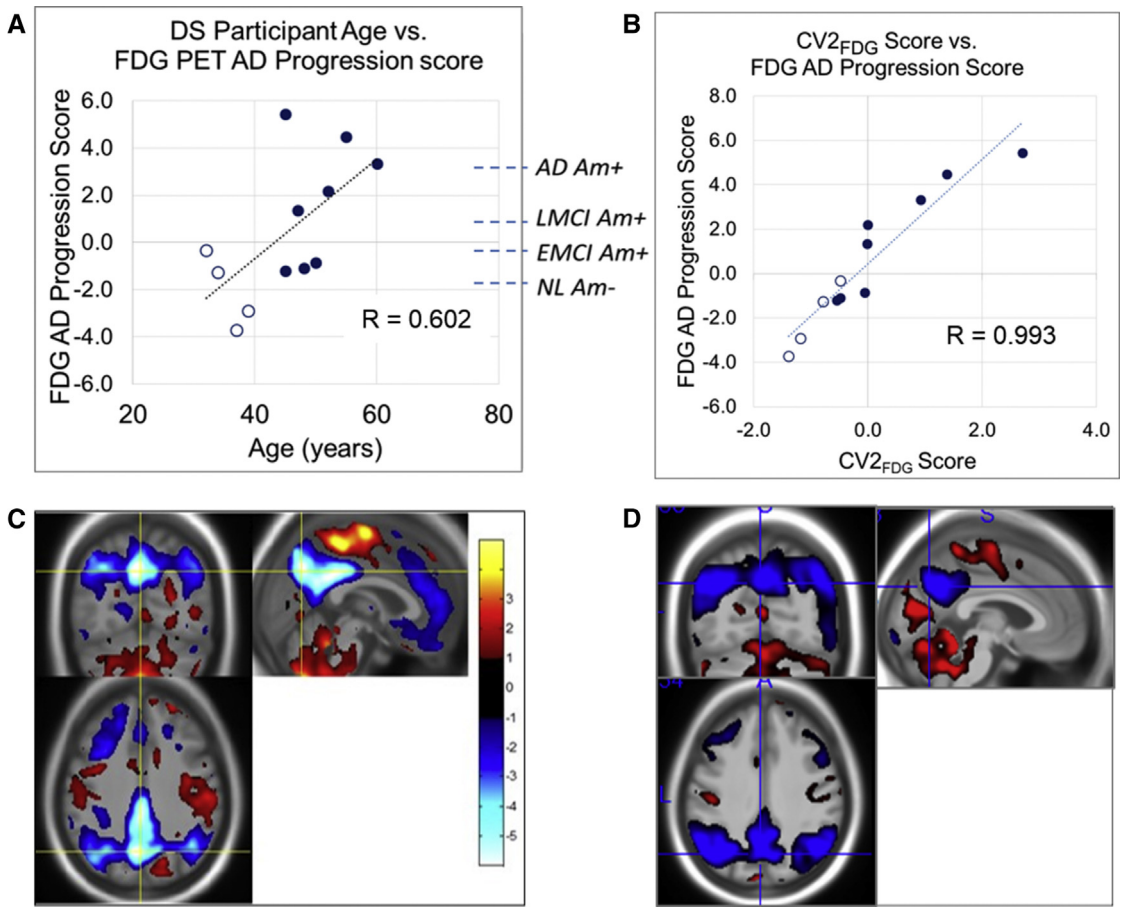

Fig. 2. Comparison of FDG AD progression classifier and $CV2_{FDG}$. (A) AD progression scores of Down syndrome subjects and correlation with subject age are plotted. Dotted lines show mean AD progression scores of independently tested amyloid-characterized subjects from the ADNI database as references (NL = cognitively normal amyloid negative, EMCI = early MCI, LMCI = late MCI); (B) Relationship between three-class FDG PET $CV2_{FDG}$ scores and FDG AD progression scores; (C) FDG PET AD progression classifier pattern (eigenimage); (D) $CV2_{FDG}$ pattern. Blue = relative hypometabolism, Red = relative hyper or preserved metabolism. Abbreviation: FDG, fluorodeoxyglucose; PET, positron emission tomography; DS, Down syndrome; AD, Alzheimer's disease; ADNI, Alzheimer's Disease Neuroimaging Initiative.

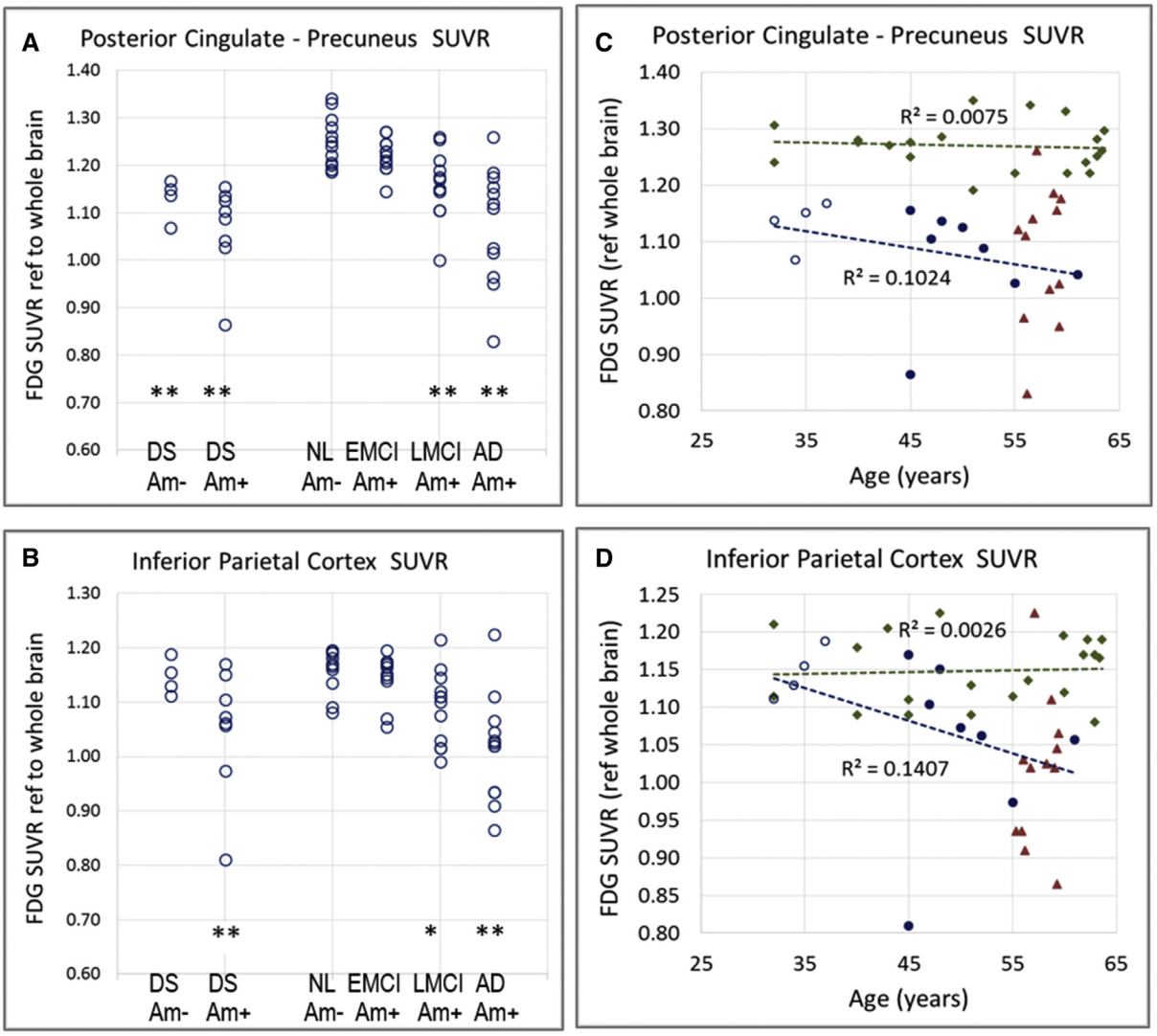

Fig. 3. FDG PET region of interest results. The posterior cingulate-precuneus (A) and inferior parietal cortex (B) region of interest SUVR values are shown, normalized to whole brain, for DS Am−, DS Am+, NL Am−, EMCI Am+, LMCI Am+, and AD Am+ subjects. Asterisks indicate nonparametric comparison test (Wilcoxon−Mann−Whitney) significance levels (*$P < .05$, **$P < .005$, tr = trend). $P < .005$ remained significant after Bonferroni correction for multiple comparisons. In c and d, relationships between regional SUVR values and age are shown for DS, NL (green diamonds), and AD subjects (red triangles). For the DS subjects in (C) and (D), unfilled circles are amyloid negative or threshold, and filled circles are amyloid positive. Abbreviation: FDG, fluorodeoxyglucose; PET, positron emission tomography; DS, Down syndrome; NL = cognitively normal amyloid negative, EMCI, early MCI; LMCI, late MCI; AD, Alzheimer's disease.

in $CV1_{FDG}$ and $CV2_{FDG}$, regional PCC was lower than NL in both DS Am− and DS Am+ (both $P < .005$) subjects and decreased with age. In contrast, DS Am− subjects did not differ from NL in IPL, whereas DS Am+ showed an age-associated trajectory toward LMCI and AD levels. Consistent with NPAIRS results, hypometabolism was also measured in Hippocampus. Results were consistent when comparing to AE-NLs and when using pons as a comparative reference region (Supplementary Table 1).

3.5. Correlation between PET markers and cognitive/functional measures

Fig. 4 shows example correlation plots between clinical endpoints and $CV2_{FDG}$ scores (4a) and amyloid SUVR (4b) in DS subjects. $CV2_{FDG}$ score correlates with several baseline measures including Observer Memory Questionnaire-Parent Form (OMQ-PF [44], R = −0.776, $P < .003$), attention (R = −0.776, $P < .003$), daily living skills (R = −0.690, $P < .01$), total memory (R = −0.627, $P < .03$), and CAMCOG total errors (R = 0.595, $P < .04$), and at trend level with CAMCOG total score 2 (composite of orientation, language, remote memory, recent memory, attention, abstraction, perception, R = −0.524, $P < .08$; Fig. 4A). $CV1_{FDG}$ correlates with baseline Communication score (R = −0.680, $P < .02$). In contrast, although Am− status corresponds to better cognitive and functional scores than Am+ status and reaches significance for OMQ-PF (R = −0.680, $P < .02$), there is no correlation between amyloid

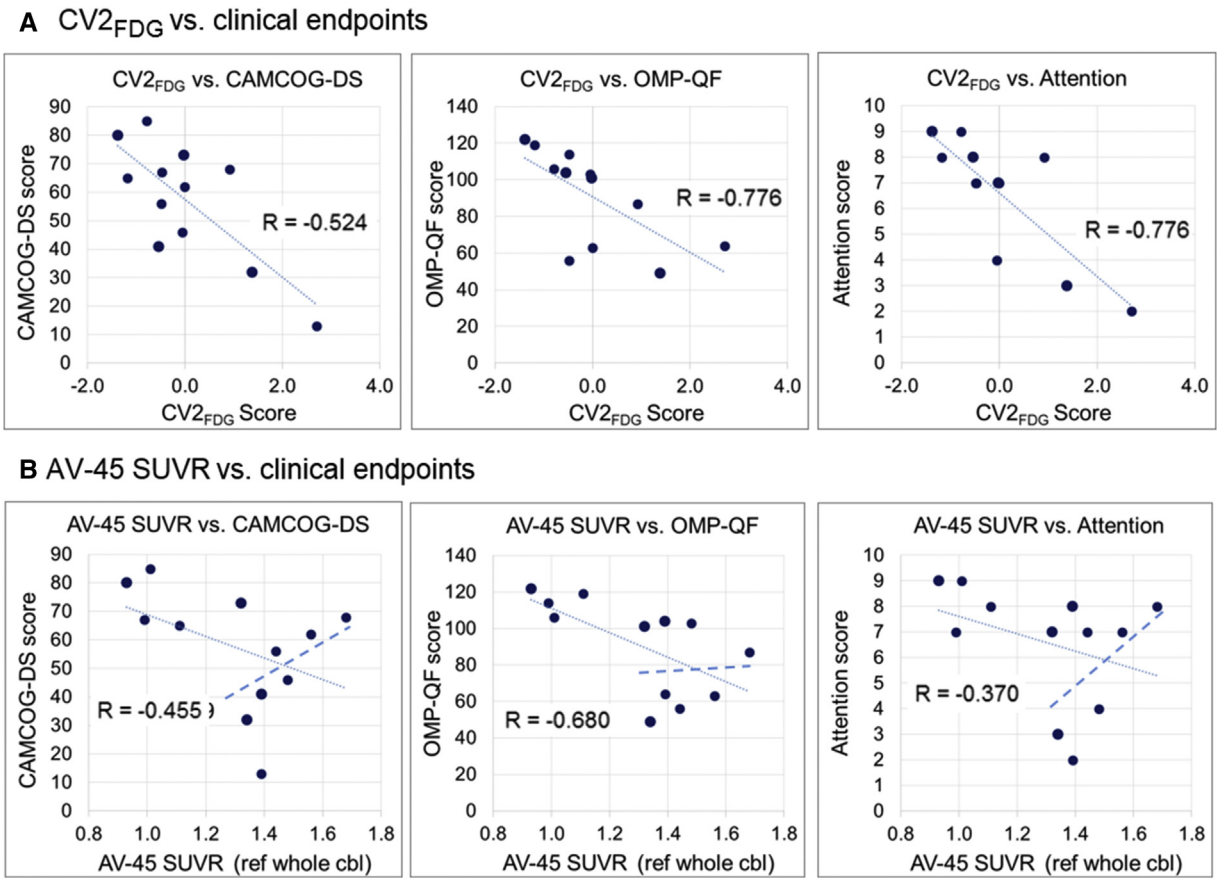

Fig. 4. Correlations between FDG and amyloid PET measures and clinical data. (A) $CV2_{FDG}$ score in DS subjects vs cognitive and functional measures at baseline, and (B) Amyloid SUVR in DS subjects vs cognitive and functional measures at baseline. The FDG values correlate with clinical endpoints throughout the spectrum of scores. In contrast, although there is a general correlation between amyloid negative vs amyloid positive status and clinical endpoints, the correlation no longer holds within the amyloid positive subgroups (second set of dotted lines). Spearman's R values are shown.

SUVR and clinical endpoints within the Am+ subset (Fig. 4B).

3.6. Structural MRI results

Fig. 5 illustrates results from the 3-class NPAIRS analysis of modulated gray MRI segments of DS, NL, and AD, which produced two CVs. The first CV (Fig. 5A, $CV1_{sMRI}$) differentiated DS from NL ($P < .00001$, ES 3.55) and AD ($P < .00001$, ES 4.87), and also contributed to discrimination between NL and AD ($P < .00002$, ES 2.09) (Wilcoxon–Mann–Whitney tests). This pattern shows DS volume reductions in cerebellum, occipital cortex, hippocampus, mid-cingulate, anterior cingulate, and temporal cortex. Preserved or increased volume was found in DS in caudate, putamen, thalamus, inferior lateral temporal cortex, inferior parietal cortex, and prefrontal cortex compared to NL and AD. AD scores were lower than NL, to interpret in combination with the second pattern (Fig. 5B, $CV2_{sMRI}$). $CV2_{sMRI}$ differentiated NL from AD ($P < .003$, ES 1.65), whereas DS scores distributed across the range from NL to AD. This pattern showed volume reductions in posterior cingulate, precuneus, parietal cortex, hippocampus, temporal cortex, frontal cortex, and caudate, with preserved or increased volume in putamen, thalamus, and midbrain. Volume reductions were consistent with AD-like atrophy.

As in $CV1_{FDG}$, there is no association between $CV1_{sMRI}$ score and amyloid status or age in DS subjects. As in $CV2_{FDG}$, four of six subjects with the lowest $CV2_{sMRI}$ scores are Am− or threshold.

As a caveat, some scans had motion artifact that introduced noise into the analyses. One scan was excluded from analyses in Figs. 4 and 5 due to blur. Three Am+ DS subjects showed notable ventricular enlargement. In addition, whereas DS scans were acquired on a 1.5 T scanner and ADNI comparator scans came from a combination of 1.5 T and 3 T scanners, no resolution-related patterns were identified using the smoothed gray matter segments.

The DS sMRI CV scores showed somewhat weaker relationships with clinical measures than FDG CV scores. $CV2_{sMRI}$ scores correlate with OMQ-PF ($R = -0.718$, $P < .01$, Fig. 5E), Attention ($R = -0.636$, $P < .04$), Total Memory ($R = -0.573$, $P < .06$, trend), and Daily Living

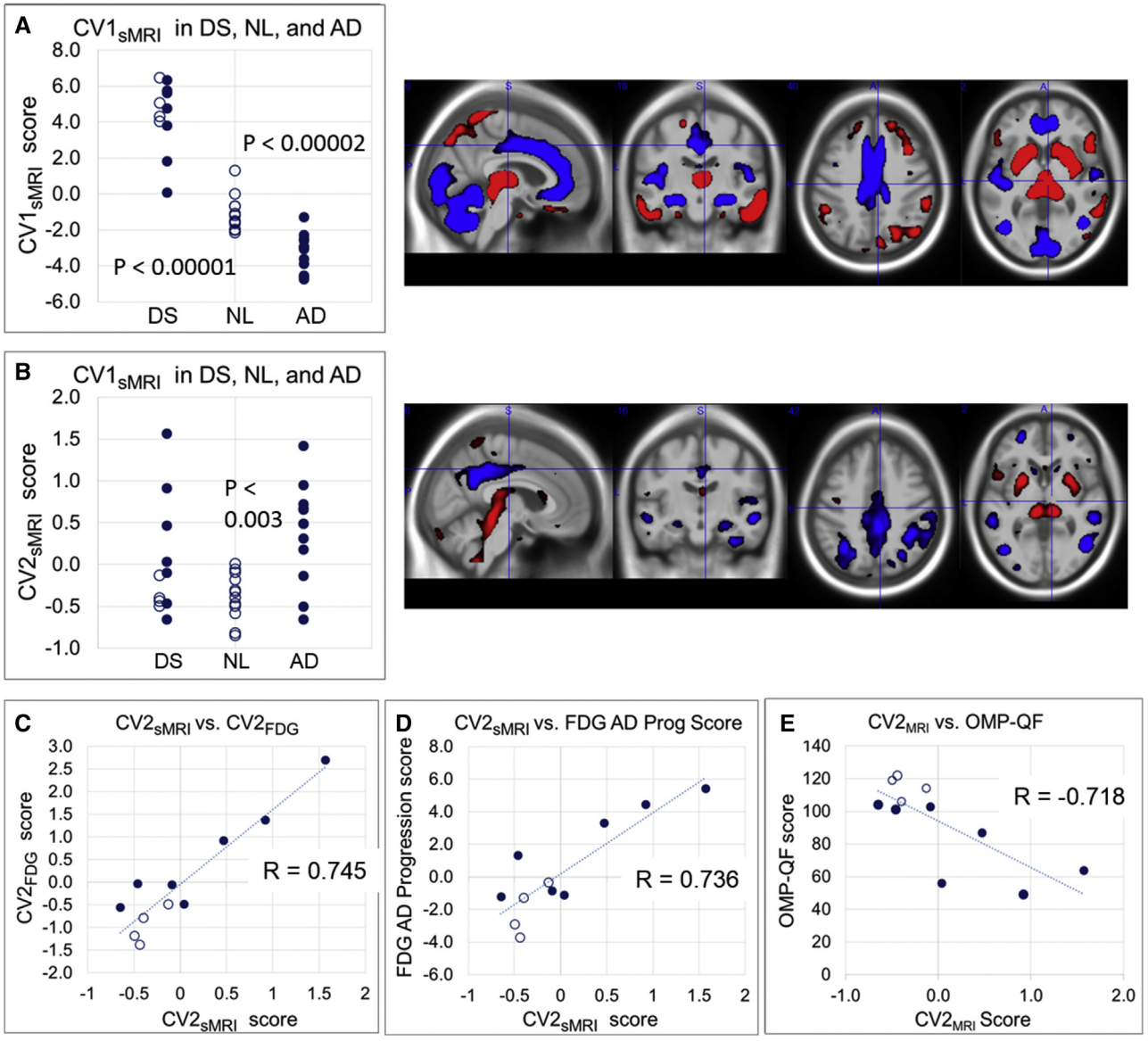

Fig. 5. Structural MRI analysis results. (A) Down syndrome associated pattern ($CV1_{sMRI}$) and (B) AD associated pattern derived from the three-class MRI NPAIRS analysis. The numeric score for each subject (circle) reflects the degree to which they express the corresponding pattern of relatively lower volume (blue) and greater volume (red). A higher y-axis score corresponds to greater pattern expression. Unfilled circles = amyloid negative, filled circles = amyloid positive. DS subjects who were amyloid negative or threshold are shown as unfilled circles to the left of the DS Am + subjects (filled circles). Both patterns contain elements that combine to differentiate NL and AD. (C)–(E) show correlations (Spearman's R values) between $CV2_{sMRI}$ scores vs $CV2_{FDG}$ scores, FDG AD progression scores, and OMQ-PF score, respectively.

Skills ($R = -0.560$, $P < .07$, trend). Significant correlations were not found between $CV1_{sMRI}$ scores and clinical measures.

3.7. Conjunction of functional and structural results

The $CV2_{sMRI}$ score correlates with $CV2_{FDG}$ ($R = 0.745$, $P < .008$; Fig. 5C) and AD Progression Score ($R = 0.736$, $P < .01$; Fig. 5D). Common regions between $CV1_{FDG}$ and $CV1_{sMRI}$ include relative hypometabolism and volume reduction in mid-cingulate, anterior cingulate, paracentral lobule, and hippocampus; relative hypermetabolism and volume preservation in prefrontal cortex; and relative hypermetabolism but volume reduction in occipital cortex. Common regions between $CV2_{FDG}$ and $CV2_{sMRI}$ include relative hypometabolism and reduced volume in posterior cingulate, precuneus, inferior parietal cortex, and hippocampus; and relative hypermetabolism and volume preservation in putamen and thalamus.

There were some differences between the FDG and sMRI findings. Cerebellar volume reduction was seen in DS compared to NL and AD, but metabolic differences were subtle. Volume preservation in thalamus, striatum, and lateral inferior temporal cortex was found in DS

compared to NL, but metabolic differences were not observed within FDG-CV1. Medial frontal hypermetabolism was found in DS relative to NL and AD but without volumetric preservation.

4. Discussion

In this study, while on a preliminary basis given the small sample size and other limitations, we have demonstrated the dissociation of functional and structural effects associated with adult DS independent of a positive amyloid PET scan from those associated with prodromal AD within Am+ subjects. Results also show that the degree of Alzheimer's-type neurodegeneration, reflected in FDG and MRI biomarkers, can be quantified in nondemented DS subjects. AD pattern expression varies greatly within the Am+ DS subjects as do clinical manifestations, underscoring the importance of characterization. We have also shown that FDG and MRI CV scores correlate with cognitive and functional endpoints, whereas amyloid burden does not within the Am+ DS subgroup.

The DS-associated $CV1_{FDG}$ pattern hypometabolism partially overlapped but was distinct from the AD-like $CV2_{FDG}$ pattern. Hypometabolism in paracentral lobule and striatum and prominent anterior cingulate and inferior frontal regions differed from core AD features. The mid- and anterior cingulate regions of $CV1_{FDG}$ have been associated with motor activation, error detection, and emotion [45]. Of interest is the posterior cingulate-precuneus hypometabolism in all DS subjects in NPAIRS and ROI results, significantly lower than NL and also EMCI Am+ subjects even in DS subjects negative for amyloid burden. Decreased posterior cingulate metabolism has been found in asymptomatic *APOE* ε4 carriers [8] and in some subjects with decreasing Abeta CSF but negative amyloid PET. As two of three Am− subjects and the threshold Am DS subject were not *APOE* ε4 carriers, the hypometabolism could potentially arise from trisomy-driven abnormal amyloid turnover resulting in excess accumulation of Abeta rather than *APOE* ε4 effects or another mechanism. We note that all subjects had positive retinal amyloid measures [3]. Similar hypometabolism was seen in hippocampus in the NPAIRS and region of interest results when referenced to pons. Study of subjects in their 20's could enable investigation of the point at which hypometabolism in these regions begins to appear.

The relative frontal hypermetabolism within $CV1_{FDG}$ was consistent with reports of regional hypermetabolism in young DS subjects. Such studies have hypothesized compensatory activity in response to deficient neural networks [12,13,15,46] and/or a lower effectiveness of glycolysis related to downregulation of phosphoglucose isomerase, elevating glucose-6-phosphate [13].

The AD-like FDG pattern ($CV2_{FDG}$) is consistent with our FDG AD progression pattern and AD literature, supporting AD-relevance, and robustness despite small sample size. As in ADNI subjects, the AD-like pattern in DS subjects correlates with clinical endpoints. The presence of AD-like effects in nondemented DS is consistent with findings of an AD-like pattern in older nondemented DS by Azari [47]. The posterior cingulate hypometabolism in this pattern was consistent with findings by Sabbagh et al in both nondemented and demented DS, correlating with increasing age and dementia [17].

DS-specific pattern $CV1_{sMRI}$ is consistent with reports of reduced cerebellar, cingulate, and hippocampal volume but preserved or increased subcortical volume, whereas $CV2_{sMRI}$ was consistent with AD-related atrophy. As $CV1_{sMRI}$ also captured differences between NL and AD, further exploration of the relationship between the two CVs is merited.

FDG and sMRI findings showed similarities and differences in the patterns differentiating DS from normals. Of note is the cerebellum, involved in motor and postural control, affected in DS [48]. Despite reduced cerebellar volume in DS compared to NL, cerebellar hypometabolism was subtle. Relevant DS murine model work has found that despite reduced volume and cell density, there were no synaptic plasticity deficits to which motor deficits could be attributed [48]. Our findings suggest that structural and functional imaging information may be complementary.

There were limitations to this pilot study, particularly in the small sample size. The NPAIRS software aided in addressing this through its segregation of signal from background noise and prevention of model over-fitting through iterative resampling. However, additional subjects will be important for confirmation and further pattern characterization. Although the sourcing of DS subjects from a single site (UCSD) and the primary ADNI comparators from multiple other sites was another potential limitation, analyses specifically comparing ADNI subjects from the DS site showed no site-specific differences. Although age differences were also a limitation, the consistency of NPAIRS results obtained when age-matched NYU subjects were included, and when explicitly comparing ROIs between DS subjects and nearly identically age-matched NL-AE subjects, suggests that patterns were not due to age differences. Related to age, although no age correlation was observed in the DS-specific CV1 patterns, the youngest subject in this study was aged 32 years. Studying adults in their late teens and twenties may help to resolve the contrast between hypometabolism observed in our subjects and the hypermetabolism-only findings of some studies in young subjects, by filling this data gap. The cross-sectional study paradigm was also a limitation, partially offset by inclusion of multiple comparator classes with progressive stages of disease severity and our observation of consistent longitudinal increases in AD progression pattern expression in Am+ ADNI subjects. Longitudinal data anticipated through studies such as DSBI and the Neurodegeneration in Aging Down Syndrome study (NiAD) could help to

expand on this work. In particular, findings would be supported if CV2 AD-like patterns are increasingly expressed in Am+ DS subjects over time, whereas the DS related CV1 patterns remain stable. Despite these various constraints, several elements support the validity of our findings, including the reproducibility and prediction metrics generated by NPAIRS, the alignment of AD-like pattern expression with amyloid positivity, the high correlation between AD-like pattern expression and relevant clinical measures, and consistency with published data from other studies.

The ability to dissociate functional and structural effects arising from AD vs underlying DS phenomena and to quantify degree of AD progression may enable identification of subjects likely to progress within a trial and detection of disease-specific treatment response. These capabilities could significantly enhance the viability of clinical trials of AD-targeted therapies in DS adults.

Acknowledgments

We acknowledge and thank Janssen Research and Development for their support of the study data acquisition, the ADCS for their role in the original image data QC, Craig Pennington of ADM Diagnostics for his instrumental role in the project collaboration, and the Alzheimer's Disease Neuroimaging Initiative and New York University for data used in comparison analyses. The development of the AD progression classifier by ADM Diagnostics was funded in part by SBIR grant award IIP-1256638 from the National Science Foundation.

Data collection and sharing for the ADNI comparator subjects used in this project was funded by the Alzheimer's Disease Neuroimaging Initiative (ADNI) (National Institutes of Health Grant U01 AG024904) and DOD ADNI (Department of Defense award number W81XWH-12-2-0012). ADNI is funded by the National Institute on Aging, the National Institute of Biomedical Imaging and Bioengineering, and through generous contributions from the following: AbbVie, Alzheimer's Association; Alzheimer's Drug Discovery Foundation; Araclon Biotech; BioClinica, Inc.; Biogen; Bristol-Myers Squibb Company; CereSpir, Inc.; Eisai Inc.; Elan Pharmaceuticals, Inc.; Eli Lilly and Company; EuroImmun; F. Hoffmann-La Roche Ltd and its affiliated company Genentech, Inc.; Fujirebio; GE Healthcare; IXICO Ltd.; Janssen Alzheimer Immunotherapy Research & Development, LLC.; Johnson & Johnson Pharmaceutical Research & Development LLC.; Lumosity; Lundbeck; Merck & Co., Inc.; Meso Scale Diagnostics, LLC.; NeuroRx Research; Neurotrack Technologies; Novartis Pharmaceuticals Corporation; Pfizer Inc.; Piramal Imaging; Servier; Takeda Pharmaceutical Company; and Transition Therapeutics. The Canadian Institutes of Health Research is providing funds to support ADNI clinical sites in Canada. Private sector contributions are facilitated by the Foundation for the National Institutes of Health (www.fnih.org). The grantee organization is the Northern California Institute for Research and Education, and the study has been coordinated by the Alzheimer's Disease Cooperative Study at the University of California, San Diego. ADNI data are disseminated by the Laboratory for Neuro Imaging at the University of Southern California.

Author contributions: D.C.M. was responsible for analysis design, a portion of analyses, and primary authorship. M.S.R. was the study PI and responsible for overall study design in collaboration with S.N. and W.C.M. A.S.L. performed the NPAIRS analyses of the data using software jointly designed and developed with M.N.W. and S.C.S. M.E.S., M.N.W., and S.C.S. assisted in article writing and review. R.D.A. and B.M. performed image data quality control and processing. J.B. was responsible for image acquisition, raw data quality control, and transmission. R.A.R. was responsible for fluid biomarker collection and analyses. L.M. provided age-matched cognitively normal subjects and participated in the writing of the article. Data used in the preparation of this article were obtained from the Down Syndrome Biomarker Initiative, the Alzheimer's Disease Neuroimaging Initiative database (adni.loni.usc.edu), and New York University.

Supplementary data

Supplementary data related to this article can be found at http://dx.doi.org/10.1016/j.trci.2016.02.004.

RESEARCH IN CONTEXT

1. Systematic review: The authors reviewed the literature using PubMed and meeting abstracts. Relevant studies inclusive of early imaging research through current year work were incorporated into background preparation and are appropriately cited.
2. Interpretation: Our findings led to new insights dissociating and quantifying the glucose metabolic and volumetric effects of Down syndrome and Alzheimer's disease within the same subjects and their relationship to amyloid burden and clinical status.
3. Future directions: The article lays groundwork for expanded studies to understand the contributions of DS and AD to clinical phenotype and to evaluate disease-specific interventional effects. Additional work could include the following: the study of a larger number of DS subjects to confirm results; the study of DS subjects from late teens through late twenties to identify potential changes occurring in earliest adulthood; longitudinal evaluation to identify AD-related changes differentiable from DS effects.

References

[1] Head E, Powell D, Gold BT, Schmitt FA. Alzheimer's Disease in DS. Eur J Neurodegener Dis 2012;1:353–64.

[2] Ness S, Rafii M, Aisen P, Krams M, Silverman W, Manji H. Down's syndrome and Alzheimer's disease: towards secondary prevention. Nat Rev Drug Discov 2012;11:655–6.

[3] Rafii MS, Wishnek H, Brewer JB, Donohue MC, Ness S, Mobley WC, et al. The Down Syndrome Biomarker Initiative (DSBI) Pilot: Proof of Concept for Deep Phenotyping of Alzheimer's Disease Biomarkers in Down Syndrome. Front Behav Neurosci 2015;9:239.

[4] Drzezga A, Lautenschlager N, Siebner H, Riemenschneider M, Willoch F, Minoshima S, et al. Cerebral metabolic changes accompanying conversion of mild cognitive impairment into Alzheimer's disease: a PET follow-up study. Eur J Nucl Med Mol Imaging 2003; 30:1104–13.

[5] Mosconi L, Mistur R, Switalski R, Tsui WH, Glodzik L, Li Y, et al. FDG-PET changes in brain glucose metabolism from normal cognition to pathologically verified Alzheimer's disease. Eur J Nucl Med Mol Imaging 2009;36:811–22.

[6] Minoshima S, Frey KA, Foster NL, Kuhl DE. Preserved pontine glucose metabolism in Alzheimer disease: a reference region for functional brain image (PET) analysis. J Comput Assist Tomogr 1995; 19:541–7.

[7] Reiman EM, Caselli RJ, Yun LS, Chen K, Bandy D, Minoshima S, et al. Preclinical evidence of Alzheimer's disease in persons homozygous for the epsilon 4 allele for apolipoprotein E. N Engl J Med 1996; 334:752–8.

[8] Protas HD, Chen K, Langbaum JB, Fleisher AS, Alexander GE, Lee W, et al. Posterior cingulate glucose metabolism, hippocampal glucose metabolism, and hippocampal volume in cognitively normal, late-middle-aged persons at 3 levels of genetic risk for Alzheimer disease. JAMA Neurol 2013;70:320–5.

[9] Benzinger TL, Blazey T, Jack CR Jr, Koeppe RA, Su Y, Xiong C, et al. Regional variability of imaging biomarkers in autosomal dominant Alzheimer's disease. Proc Natl Acad Sci U S A 2013;110:E4502–9.

[10] Alexander GE, Chen K, Pietrini P, Rapoport SI, Reiman EM. Longitudinal PET evaluation of cerebral metabolic decline in dementia: A potential outcome measure in Alzheimer's disease treatment studies. Am J Psychiatry 2002;159:738–45.

[11] Head E, Silverman W, Patterson D, Lott IT. Aging and DS. Curr Gerontol Geriatr Res 2012;2012:412536.

[12] Head E, Lott IT, Patterson D, Doran E, Haier RJ. Possible compensatory events in adult DS Brain prior to the Development of Alzheimer Disease neuropathology: Targets for non-pharmacological intervention. J Alzheimers Dis 2007;11:61–76.

[13] Lengyel Z, Balogh E, Emri M, Szikszai E, Kollar J, Sikula J, et al. Pattern of increased cerebral FDG uptake in DS patients. Pediatr Neurol 2006;34:270–5.

[14] Schapiro MB, Grady CL, Kumar A, Herscovitch P, Haxby JV, Moore AM, et al. Regional cerebral glucose metabolism is normal in young adults with DS. J Cereb Blood Flow Metab 1990;10:199–206.

[15] Haier RJ, Alkire MT, White NS, Uncapher MR, Head E, Lott IT, et al. Temporal cortex hypermetabolism in DS prior to the onset of dementia. Neurology 2003;61:1673–9.

[16] Schapiro MB, Haxby JV, Grady CL. Nature of mental retardation and dementia in DS: Study with PET, CT, and neuropsychology. Neurobiol Aging 1992;13:723–34. Review.

[17] Sabbagh MN, Chen K, Rogers J, Fleisher AS, Liebsack C, Bandy D, et al. Florbetapir PET, FDG PET, and MRI in DS individuals with and without Alzheimer's dementia. Alzheimers Dement 2015; 11:994–1004.

[18] Thompson PM, Mega MS, Woods RP, Zoumalan CI, Lindshield CJ, Blanton RE, et al. Cortical change in Alzheimer's disease detected with a disease-specific population-based brain atlas. Cereb Cortex 2001;11:1–16.

[19] Risacher SL, Shen L, West JD, Kim S, McDonald BC, Beckett LA, et al. Longitudinal MRI atrophy biomarkers: Relationship to conversion in the ADNI cohort. Neurobiol Aging 2010;31:1401–18.

[20] Dukart J, Mueller K, Villringer A, Kherif F, Draganski B, Frackowiak R, et al., Alzheimer's Disease Neuroimaging Initiative. Relationship between imaging biomarkers, age, progression and symptom severity in Alzheimer's disease. Neuroimage Clin 2013; 3:84–94.

[21] Smits LL, Tijms BM, Benedictus MR, Koedam EL, Koene T, Reuling IE, et al. Regional atrophy is associated with impairment in distinct cognitive domains in Alzheimer's disease. Alzheimers Dement 2014;10(5 Suppl):S299–305.

[22] Nho K, Risacher SL, Crane PK, DeCarli C, Glymour MM, Habeck C, et al., Alzheimer's Disease Neuroimaging Initiative–ADNI. Voxel and surface-based topography of memory and executive deficits in mild cognitive impairment and Alzheimer's disease. Brain Imaging Behav 2012;6:551–67.

[23] Pinter JD, Eliez S, Schmitt JE, Capone GT, Reiss AL. Neuroanatomy of Down's Syndrome: A high-resolution MRI study. Am J Psychiatry 2001;158:1659–65.

[24] Carducci F, Onorati P, Condoluci C, De Gennaro G, Quarato PP, Pierallini A, et al. Whole-brain voxel-based morphmetry study of children and adolescents with DS. Funct Neurol 2013;28:19–28.

[25] Smigielska-Kuzia J, Boćkowski L, Sobaniec W, Sendrowski K, Olchowik B, Cholewa M, et al. A volumetric magnetic resonance imaging study of brain structures in children with DS. Neurol Neurochir Pol 2011;45:363–9.

[26] White NB, Alkire MT, Haier RJ. A voxel-based morphometric study of nondemented adults with DS. Neuroimage 2003;20:393–403.

[27] Pearlson GD, Breiter SN, Aylward EH, Warren AC, Grygorcewicz M, Frangou S, et al. MRI brain changes in subjects with DS with and without dementia. Dev Med Child Neurol 1998;40:326–34.

[28] Aylward EH, Li Q, Honeycutt NA, Warren AC, Pulsifer MB, Barta PE, et al. MRI volumes of the hippocampus and amygdala in adults with Down's syndrome with and without dementia. Am J Psychiatry 1999;156:564–8.

[29] Teipel SJ, Alexander GE, Schapiro MB, Moller HJ, Rapoport SI, Hampel H. Age-related cortical grey matter reductions in nondemented Down's syndrome adults determined by MRI with voxel-based morphometry. Brain 2004;127:811–24.

[30] Raz N, Torres IJ, Briggs SD, Spencer WD, Thornton AE, Loken WJ, et al. Selective neuroanatomic abnormalities in Down's syndrome and their cognitive correlates: evidence from MRI morphometry. Neurology 1995;45:356–66.

[31] Hartley S, Handen BL, Devenney DA, Hardison R, Mihaila I, Price JC, et al. Cognitive functioning in relation to brain amyloid-B in healthy adults with DS. Brain 2014;137(Pt 9):2556–63.

[32] Handen BL, Cohen AD, Channamalappa U, Bulova P, Cannon SA, Cohen WI, et al. Imaging brain amyloid in nondemented young adults with DS using Pittsburgh compound B. Alzheimers Dement 2012; 8:496–501.

[33] Jennings D, Seibyl J, Sabbagh M, Lai F, Hopkins W, Bullich S, et al. Age dependence of brain β-amyloid deposition in DS: An [18F]florbetaben PET study. Neurology 2015;84:500–7.

[34] Lao PJ, Betthauser TJ, Hillmer AT, Price JC, Klunk WE, Mihaila I, et al. The effects of normal aging on amyloid-β deposition in nondemented adults with Down syndrome as imaged by carbon 11-labeled Pittsburgh compound B. Alzheimers Dement 2016;12:380–90.

[35] Moran JA, Rafii MS, Keller SM, Singh BK, Janicki MP, American Academy of Developmental Medicine and Dentistry; Rehabilitation Research and Training Center on Aging With Developmental Disabilities, University of Illinois at Chicago; American Association on Intellectual and Developmental Disabilities. The National Task Group on Intellectual Disabilities and Dementia Practices consensus recommendations for the evaluation and management of dementia in adults with intellectual disabilities. Mayo Clin Proc 2013;88:831–40.

[36] Strother SC, Anderson J, Hansen LK, Kjems U, Kustra R, Sidtis J, et al. The quantitative evaluation of functional neuroimaging experiments: the NPAIRS data analysis framework. Neuroimage 2002; 15:747–71.

[37] Strother SC, Oder A, Spring R, Grady C. The NPAIRS Computational Statistics Framework for Data Analysis in Neuroimaging. Proceedings of COMPSTAT'2010 pp 111–120 September 30 2010.

[38] Mormino EC, Kluth JT, Madison CM, Rabinovici GD, Baker SL, Miller BL, et al., Alzheimer's Disease Neuroimaging Initiative. Episodic memory loss is related to hippocampal-mediated β-amyloid deposition in elderly subjects. Brain 2009;132:1310–23.

[39] Landau SM, Breault C, Joshi AD, Pontecorvo M, Mathis CA, Jagust WJ, et al., Alzheimer's Disease Neuroimaging Initiative. Amyloid-β imaging with Pittsburgh compound B and florbetapir: Comparing radiotracers and quantification methods. J Nucl Med 2013;54:70–7.

[40] Shaw LM, Vanderstichele H, Knapik-Czajka M, Clark CM, Aisen PS, Petersen RC, et al., Alzheimer's Disease Neuroimaging Initiative. Cerebrospinal fluid biomarker signature in Alzheimer's disease neuroimaging initiative subjects. Ann Neurol 2009;65:403–13.

[41] Matthews DC, Davies M, Murray J, Williams S, Tsui WH, Li Y, et al. Physical activity, Mediterranean diet and biomarkers-assessed risk of Alzheimer's: A Multi-Modality Brain Imaging Study. Adv J Mol Imaging 2014;4:43–57.

[42] Strother SC, Matthews D, Lukic A, Andrews A, Wernick M. Superior Performance of a Multi-Stage PET Classifier for the Alzheimer's Disease Cascade. Organisation of Human Brain Mapping Annual Meeting [Interactive Poster 37]; 2011. Available at: https://www.researchgate.net/publication/233741172_Superior_Performance_of_a_Multi-Stage_PET_Classifier_for_the_Alzheimers_Disease_Cascade. Accessed March 15, 2016.

[43] Li Y, Rinne JO, Mosconi L, Pirraglia E, Rusinek H, DeSanti S, et al. Regional analysis of FDG and PIB-PET images in normal aging, mild cognitive impairment, and Alzheimer's disease. Eur J Nucl Med Mol Imaging 2008;35:2169–81.

[44] Gonzalez LM, Anderson VA, Wood SJ, Mitchell LA, Heinrich L, Harvey AS. The Observer Memory Questionnaire-Parent Form: introducing a new measure of everyday memory for children. J Int Neuropsychol Soc 2008;14:337–42.

[45] Beckmann M, Johansen-Berg H, Rushworth MF. Connectivity-based parcellation of human cingulate cortex and its relation to functional specialization. J Neurosci 2009;29:1175–90.

[46] Haier RJ, Head K, Head E, Lott IT. Neuro-imaging of individuals with DS at-risk for dementia: evidence for possible compensatory events. Neuroimage 2008;39:1324–32.

[47] Azari NP, Pettigrew KD, Pietrini P, Horwitz B, Schapiro MB. Detection of an Alzheimer disease pattern of cerebral metabolism in Down syndrome. Dementia 1994;5:69–78.

[48] Galante M, Jani H, Vanes L, Daniel H, Fisher EM, Tybulewicz VL, et al. Impairments in motor coordination without major changes in cerebellar plasticity in the Tc1 mouse model of DS. Hum Mol Genet 2009;18:1449–63.